Electronic structure investigation of energetics and positron lifetimes of fully relaxed monovacancies with various charge states in 3*C*-SiC and 6*H*-SiC

Julia Wiktor,[1,*] Gérald Jomard,[1] Marc Torrent,[2] and Marjorie Bertolus[1]
[1]*CEA, DEN, DEC, Centre de Cadarache, 13108, Saint-Paul-lez-Durance, France*
[2]*CEA, DAM, DIF, F-91297, Arpajon, France*
(Received 9 April 2013; published 24 June 2013)

We present first-principles calculations of formation energies of various charge states of V_C, V_{Si}, and $V_C + C_{Si}$ defects in 3*C* and 6*H* silicon carbide to predict if they can be detected by positron annihilation spectroscopy (PAS). We use the two-component density functional theory to compute positron lifetimes in both polytypes, taking into account atomic relaxation due to both the defect and the positron. Three different calculation schemes are used. We find longer lifetimes than the ones obtained in previous theoretical studies in which relaxation was not taken into account or was only estimated. For the neutral carbon vacancy, we find lifetimes from 173 ps in 6*H*-SiC to 195 ps in 3*C*-SiC, while for the silicon vacancy, we obtain lifetimes from 222 to 227 ps in both polytypes, depending on the charge state. Based on these results, we propose that some experimental positron lifetimes assigned to V_{Si} could in fact be related to defects containing V_C. In consequence, the experimental data interpretation and defect identification should be probably reconsidered.

DOI: 10.1103/PhysRevB.87.235207 PACS number(s): 71.15.Mb, 71.60.+z, 61.72.J−

I. INTRODUCTION

Silicon carbide is a ceramic with a high melting point, a good chemical stability, and a low neutron absorption. These properties make it a possible cladding material in high temperature fission reactors[1] and fusion reactors.[2] Moreover, as a wide band gap semiconductor, it is envisaged as an alternative for silicon in microelectronic devices.[3] Silicon carbide exists in different polytypes, among which the 3*C*, 4*H*, and 6*H* are the most common and the most studied.

Defects in SiC can be studied by positron annihilation spectroscopy (PAS). PAS is a powerful nondestructive technique, allowing one to probe open volume defects. As a positron gets trapped in a vacancy-type defect, its average lifetime increases and this can be measured. To identify the type of defects corresponding to a specific lifetime comparison with other characterization methods or calculated lifetimes is required. Results of PAS experiments on SiC have been already published.[4–14] However, as Lam *et al.* showed in Table I of Ref. 10, there is a high discrepancy of the experimental lifetimes attributed to monovacancies in SiC.

The interpretation of the PAS experimental results is usually based on theoretical lifetime calculations. Positron lifetimes of defects in SiC were calculated, for example, by Brauer *et al.*,[15,16] Kawasuso *et al.*,[9] and Staab *et al.*[17] However, at the time when these studies were performed, limited computational resources did not allow one to perform fully self-consistent positron lifetime calculations nor to take into account the full relaxation of defects. The positron lifetime is highly sensitive to the defect volume, and in semiconductors the volumes of relaxed and ideal vacancies differ strongly. Several authors have shown that in the case of a monovacancy in bulk Si, the atomic relaxation due to the positron should not be neglected in lifetime calculations.[18–20] The case of SiC should be similar. Up to now, the effect of the atomic relaxation on positron lifetime was only estimated for silicon carbide.[9,17]

Several positron lifetime calculations schemes exist. In our study, we consider three of them. The first one is a non-self-consistent conventional scheme, which is mostly accurate for perfect crystals. Two self-consistent schemes, GGGC[21] and PSN,[22] based on the two-component density functional theory, have also been developed. These two calculation methods allow one to fully take into account the relaxation caused by both the defect creation and the presence of the positron.

Our objective was to revisit the PAS identification of monovacancies in SiC thanks to the more sophisticated methods available nowadays. We wanted to calculate positron lifetimes for two monovacancies, V_C and V_{Si}, as well as the $V_C + C_{Si}$ complex, which has been shown to be more stable than V_{Si} in certain conditions.[23,24] We performed our calculations for two polytypes of silicon carbide: 3*C*-SiC and 6*H*-SiC. Additionally, we investigated the formation energies of different charge states of the defects. It allowed us to predict if they are stable and if they can be detected by PAS.

This paper is organized as follows. In Sec. II, we present the methods used for formation energy calculations and the three positron lifetime calculation schemes. In Sec. III, we describe the computational details, as well as the results of the preliminary studies that allowed us to choose the parameters used in the calculations. In Sec. IV, we present our results of formation energies and positron lifetimes of neutral and charged defects in both 3*C*-SiC and 6*H*-SiC. Finally, in Sec. V, we compare the positron lifetimes yielded by our calculations with the experimental lifetimes from the literature.

II. METHOD

A. Defects charge states and formation energies

The charge of a defect determines if it can be detected by PAS. Positive vacancies should not be observed as they create a long-range repulsive Coulomb potential, which results in a small trapping coefficient. Negative and neutral vacancies, on the contrary, can be observed and distinguished as the trapping coefficient of the negative vacancies decreases with temperature while it is constant for the neutral ones.[25] It is therefore important to consider the various possible charge states of each defect. Our formation energy calculations were

performed for charge states varying from -2 to $+2$. This was done to predict if the given monovacancy can be detected by PAS and to know which charge state can be expected in the examined samples. To calculate the formation energy of charged defects, we used a formula based on a standard formalism proposed by Zhang and Northrup for GaAs[26] and adapted by Zywietz, Furthmüller, and Bechstedt[27] for SiC. The basic equation describing the defect formation energy E_f reads[23]

$$E_f(V_X,q) = E_{tot}(V_X,q) - n_C\mu_C - n_{Si}\mu_{Si} + q\mu_e, \quad (1)$$

where $E_{tot}(V_X,q)$ is the total energy of the supercell, n_C and n_{Si} are the numbers of carbon and silicon atoms in the cell, μ_C and μ_{Si} are the chemical potentials of the carbon and the silicon atom in SiC, q is the charge of the defect, and μ_e is the electron chemical potential, which varies from the bottom to the top of the band gap. However, we cannot directly use Eq. (1). Approximations have to be used to determine the formation energy. Firstly, because the chemical potentials of carbon and silicon atoms in SiC are not known. Secondly, the classical supercell approach fails in providing accurate formation energies for charged supercells. Even if a large number of atoms is used in calculations, the defects cannot be considered as isolated because of the long-range electrostatic interactions. Various schemes of energy correction were proposed.[28–30] To minimize the numerical errors and to approximate the values of μ_C and μ_{Si}, we chose to use the following formula to calculate the formation energy:

$$\begin{aligned} E_f(V_X,q) = {} & E_{tot}(V_X,q) - n_C\mu_{SiC}^{bulk} \\ & - (n_{Si} - n_C)\left[\mu_{Si}^{bulk} + \frac{1}{2}\Delta H_f(SiC)\right] \\ & + q(E_{VBM} + \mu_e + \Delta V) + \frac{2}{3}\Delta E_{el}(q), \quad (2) \end{aligned}$$

where E_{tot} is the energy of the supercell with a defect, μ_{SiC}^{bulk} is the energy per SiC pair in a perfect material, and μ_{Si}^{bulk} is an energy per atom in bulk silicon. ΔH_f is the formation enthalpy, calculated as

$$\Delta H_f(SiC) = \mu_{SiC}^{bulk} - \mu_{Si}^{bulk} - \mu_C^{bulk}, \quad (3)$$

with μ_C^{bulk}, an energy per carbon atom in diamond structure. E_{VBM} is the energy of the valence-band maximum in the perfect cell. ΔE_{el} is known as the Madelung correction, which was proposed by Leslie and Gillan.[28] It is a simple electrostatic correction, introducing a monopole term ΔE_{el},

$$\Delta E_{el} = \frac{\alpha q^2}{2\epsilon_0 L}, \quad (4)$$

where α is the Madelung lattice constant, ϵ is the static dielectric constant and L is the length of the supercell edge. ΔE_{el} tends to overestimate the correction, as it takes into account only the monopole term of the electrostatic interaction. Therefore we used an improved scheme proposed by Lany and Zunger,[29] which contains only 2/3 of the Madelung term, along with a potential alignment ΔV. To calculate the ΔV, the method proposed by Taylor and Bruneval[30] taking

$$\Delta V = \langle v_{KS}^{bulk}\rangle - \langle v_{KS}^{defect}\rangle, \quad (5)$$

was used. $\langle v_{KS}^{bulk}\rangle$ and $\langle v_{KS}^{defect}\rangle$ are the average Kohn-Sham potentials calculated for the cell without and with the defect, respectively.

The formation energies of charged defects change with the electron chemical potential μ_e, but DFT is known to fail in predicting its range. For example, we find gaps of 1.35 eV for 3C-SiC and of 2.01 eV for 6H-SiC, while the experimental gaps are equal to 2.36 eV and 3.0 eV,[31] respectively. Some authors vary μ_e up to the experimental conduction-band minimum. We chose to plot our results only up to the theoretical band gap edge to be consistent with the method used. Our μ_e cannot hence be directly compared with the experimental one. It is rather an indication of the position of the chemical potential in the band gap and cannot be used as a quantitative estimation of the ionization levels of the vacancies. Also, the band gap error can affect the positions of the charge transition levels.[33]

Additionally, it has to be noted that no perfect way to correct the effects of finite cell sizes nor of the too small gap calculated in DFT is known. It was also proposed that none of the corrections is accurate when dealing with defect states that are hybridized with band edges.[32] Thus the formation energies and ionization levels presented here should be used with caution, even though corrections were used.

B. Positron lifetime calculations

To calculate the lifetime of a positron, it is necessary to know how its density is distributed in the system and at which points of space there is a probability of annihilation with an electron. The positron lifetime τ depends hence on both the positron ground-state density $n^+(\boldsymbol{r})$ and the electron ground-state density $n(\boldsymbol{r})$ and can be calculated as an inverse of a trapping rate λ:

$$\frac{1}{\tau} = \lambda = \pi c r_0^2 \int_{\mathbb{R}^3} d^3\boldsymbol{r}\, n^+(\boldsymbol{r}) n(\boldsymbol{r}) g(n^+,n), \quad (6)$$

where c is the speed of light and r_0 is the classical radius of an electron. The $g(n^+,n)$ term is an enhancement factor taking into account an increase in the electron density at the positron site caused by the screening of this particle by electrons.

To find the positron lifetime, one needs to know both electron and positron densities. Their distributions can be calculated using various approximations, which leads to several calculation schemes. In our study, we considered three methods, the simplest conventional scheme (CONV), the method proposed by Giglien, Galli, Gygi, and Car (GGGC)[21] and the scheme based on Boroński and Nieminen[34] calculation method, with a parametrization by Puska, Seitsonen, and Nieminen (PSN).[22] The three methods are described in Ref. 22 and we will give here only their main features.

The CONV scheme is based on the normal one-component density functional theory. Two steps of computations are done in this method (presented in the left column of Fig. 1). First, the ground-state electronic density is calculated. Then, the positron density is determined, taking into account the electron distribution. After these two steps, the positron lifetime is calculated. For the electron-positron correlation functional, the LDA zero-positron-density limit parametrized by Arponen and Pajanne[35] and provided by Boroński and Nieminen[34] is

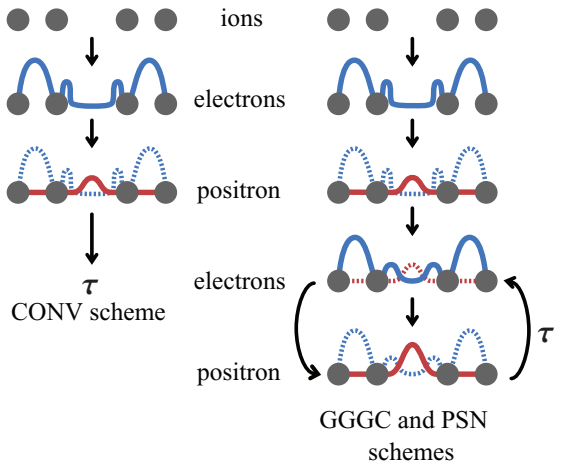

FIG. 1. (Color online) Positron lifetime calculations schemes. In the CONV scheme, only two steps are performed: the first one to find the electron density and the second one to obtain the positron density. Then, the lifetime is calculated. In the GGGC and PSN schemes, the steps are repeated until convergence is reached.

used. For the enhancement factor g, the form depending only on the electron density, modeled by Boroński and Nieminen, was taken.[34] This method is accurate for the perfect lattice as in this case the positron is delocalized and therefore does not affect the electron density. In the case of defects, however, the positron can localize and its influence on electrons cannot be neglected any longer. This can be taken into account in the GGGC and PSN schemes.

GGGC and PSN schemes are based on the two-component density functional theory (TCDFT).[25,34,36] In these methods, several self-consistent computation steps are performed, as presented in the right column of Fig. 1. First, the electron density is calculated, then the density of a positron interacting with the electrons. Later, the electron density affected by the positron is recalculated and then steps are repeated until convergence is reached.

The two self-consistent schemes use different approximations and parametrizations. The GGGC scheme uses the same parametrization as the conventional scheme, i.e., an LDA zero-positron-density limit for the electron-positron correlation functional and an enhancement factor that depends on the electron density only. In the PSN scheme, a full LDA electron-positron correlation functional provided by Puska, Seitsonen, and Nieminen[22] is used. The enhancement factor in this scheme depends on both the electron and the positron densities.

The positron lifetime is most sensitive to the available volume. In semiconductors, when a defect is created, the surrounding atoms can move relatively far away from their perfect positions. Additionally, a positron that is localized in the vacancy can repel the neighboring positive ions. In the calculations of positron lifetime of defects in SiC published so far,[9,15–17] this effect was not fully taken into account. Changes in defect volumes lead to highly different positron lifetimes. Some authors tried to estimate the relaxation effect by performing calculations in geometries already relaxed without a positron.[9,17] Our calculations were started with the perfect positions of the atoms. Then, calculations using the GGGC and PSN schemes were performed. After reaching the convergence for electron and positron densities, forces acting on ions were calculated using the Hellman-Feynman theorem. Ions were moved according to those forces and the procedure was repeated until all the forces could be neglected.

C. Enhancement factor in semiconductors

The enhancement factor g mentioned in the previous section describes the increase in the electron density at a positron site due to the screening of the positron by electrons. The forms of this factor were initially parametrized for metallic materials, in which the screening is perfect. In semiconductors and insulators, however, this effect is reduced, because of the gap in the electron energy levels. As our study is dedicated to silicon carbide, this imperfection of screening had to be taken into account.

There are two ways of correcting the enhancement factor in semiconductors. A semiconductor correction (SC) can be implemented in the enhancement factor as proposed by Puska.[37] Alternatively, a gradient correction (GC) proposed by Barbiellini *et al.*[38] can be implemented in both the enhancement factor and the electron-positron correlation energy. We decided to use the first method since the gradient correction has not yet been implemented for the PSN scheme and we wanted to be able to make the most meaningful comparison between the three schemes.

The semiconductor correction had already been introduced in the form of enhancement factor used in the CONV and GGGC schemes.[37] It was done by including a term $(1 - 1/\epsilon_\infty)$ in the enhancement factor, where ϵ_∞ is the high frequency dielectric constant of the material. However, this modification has not yet been done for the enhancement factor used in the PSN scheme. We, therefore, modified the form given by Puska, Seitsonen, and Nieminen[22] in a similar way to what was done for CONV and GCCC. The formulation of the two enhancement factors containing semiconductor corrections is shown in Appendix.

III. COMPUTATIONAL DETAILS

A. DFT parameters of charge states calculations

All calculations presented here were performed in the ABINIT[39,40] code, which uses plane-wave or wavelet basis for wave-function representation. We used the projector augmented wave[41] (PAW) method implemented in the code. The PAW data sets were generated by the *atompaw* code.[42] In the carbon PAW data set we treated $2s$ and $2p$ levels as valence states (level $1s$ included in the frozen core region), while for silicon, we considered $3s$ and $3p$ valence states (levels $1s$, $2s$, and $2p$ included in the frozen core region), which corresponds to four valence electrons for both elements. For the electron-electron exchange correlation, the GGA functional as parametrized by Perdew, Burke, and Ernzerhof (PBE)[43] was used. We considered the spin polarization and allowed a full relaxation of the defects, at constant volume (the theoretical equilibrium volume), without symmetry conservation. The parameters used in calculations are presented in Table I. This set of parameters ensured the cell parameters and total energy convergence of less than 10^{-3} Å and 2 meV/atom,

TABLE I. Parameters used in the calculations of the formation energies of charged defects in the two considered polytypes. Madelung constants for zinc-blende and wurzite structures were taken. For the static dielectric constant of 6*H*-SiC, we use an average of experimental values in ordinary and extraordinary directions.[48]

Polytype	3*C*-SiC	6*H*-SiC
Atomic sites	216	192
Plane wave E_{cut}	700 eV	700 eV
k-point mesh	$2 \times 2 \times 2$	$4 \times 4 \times 2$
Lattice parameters	$a = b = c = 4.39$ Å	$a = b = 3.10$ Å, $c = 15.21$ Å
Band gap energy	1.35 eV	2.01 eV
Madelung constant	1.638	1.641
Dielectric constant ϵ_0	9.72	9.84

respectively. Table I also lists the parameters needed for the electrostatic correction in Equation (4). For the relaxation of the defects we used the Broyden-Fletcher-Goldfarb-Shanno minimization (BFGS).[44–47] Relaxation was stopped when all the forces acting on atoms were smaller than 0.005 eV/Å.

B. Test of ABINIT implementation

Positron lifetime calculation in the PAW method was recently implemented in the ABINIT code.[40] Therefore we firstly tested this development by comparing our results with the ones obtained by Takenaka *et al.*,[49] using the all-electron full-potential linearized augmented plane-wave method (FLAPW), the most accurate implementation of DFT available up to now. As Takenaka *et al.* did not study silicon carbide, we performed calculations for perfect silicon in similar conditions. We set $1/\epsilon_\infty = 0$ and used the experimental volume. We used the same parametrization as in Ref. 49, which is equivalent to our CONV scheme. In this case, we considered a PAW data set for silicon with $2s$, $2p$, $3s$, and $3p$ valence states, hence with 12 valence electrons and we obtained a lifetime of 209 ps, which is close to Takenaka *et al.* result of 211 ps. In addition, to test the case of a trapped state, we performed calculations for V_{Si} in bulk Si. Using the CONV scheme we obtained 217 ps for the silicon vacancy relaxed without the positron (8.3% inward relaxation in D_{2d} geometry) and 241 ps for the unrelaxed vacancy. Then we fully relaxed the defect in the GGGC scheme and found a lifetime of 271 ps. These results are consistent with those of Makkonen *et al.*[19,20] (215 ps and 272 ps for the vacancy relaxed without and with the positron, respectively). The small differences between our results and those from the reference studies indicate that the positron lifetime calculation implementation in ABINIT is reliable.

C. Basis completeness for positron wave-function description

In our calculations the same basis is used for the description of both electron and positron wave functions. However, since the natures of the electron-ion and positron-ion interactions are different, the shapes of the corresponding wave functions are not the same. As a result, in some cases, the basis used for the electron wave-function representation can be inappropriate for the positron distribution description. For example, the silicon PAW data set with $3s$ and $3p$ valence states only can be successfully used for electronic structure calculations. Yet, using this PAW data set, we calculated the lattice lifetime of bulk Si of 223 ps, which is much longer than the lifetime obtained with $2s$, $2p$, $3s$, and $3p$ valence states (209 ps). It indicates that the basis with $3s$ and $3p$ valence states may not be complete enough to properly describe the positron wave function. We therefore performed another calculation using a PAW data set treating four valence electrons, but containing additional $2s$ and $2p$ projectors. This yielded the same lattice lifetime as in the 12 valence electrons calculation. It means that the large lifetime discrepancy between cases with four and 12 valence electrons is due to the basis incompleteness. This problem was further investigated and is the subject of another publication.[50]

TABLE II. Comparison of positron lifetimes obtained in 3*C*-SiC for lattice and carbon vacancy using different PAW data sets. Relative lifetimes for the carbon vacancy were calculated according to Eq. (7).

	e-e x-c approx.	Si valence electrons	Schema	Lifetime (ps)	Relative lifetime
Lattice	LDA	4	CONV	149	
Lattice	LDA	12	CONV	144	
V_C	LDA	4	GGGC	211	42%
V_C	LDA	12	GGGC	204	42%

D. Positron lifetime calculations parameters

The effect of the frozen core approximation had to be studied as well in the case of SiC. For that purpose we compared results obtained using 4 and 12 valence electrons for silicon. We also studied the effect of the approximation taken for the electron-electron interaction. For GGA calculation, we used the same parameters as for the formation energy calculations (see Sec. III A). In LDA calculations we used the theoretical lattice parameter of 4.33 Å for 3*C*-SiC and $a = b = 3.06$ Å and $c = 15.03$ Å for 6*H*-SiC. In our calculations, we used 6.52 for the high-frequency dielectric constant ϵ_∞, which is the experimental value for 3*C*-SiC.[48] Results of this preliminary study are presented in Table II.

In the case of SiC, the differences caused the number of electrons included in the frozen core are smaller than for Si. The lattice positron lifetimes is only 5 ps smaller for 12 than for four valence electrons. The difference is slightly larger for the carbon vacancy than in the case of lattice (7 ps), however the ratio between vacancy and lattice lifetimes is the same for the two PAW data sets. It means that for calculations in SiC the use of four valence electrons for silicon is satisfactory. However, in the PSN calculations the use of four valence electrons in the Si PAW data set does not allow the calculation convergence. A more complete basis had to be used in that case.

We also compared the results obtained by other authors for SiC lattice lifetimes using one of the two possible corrections taking into account the imperfect screening in semiconductors and without any correction. These results and the methods used are summarized in Table III.

It can be noticed in Table III that the calculations using no correction give lifetimes much shorter than the experimental

TABLE III. Synthesis of the calculated lattice positron lifetimes in 3*C* silicon carbide available in literature (calculated in CONV). The type of the correction and of the basis set representation used in calculations are indicated.

	Corr.	Basis set representation	Lifetime (ps)
Experimental lifetime[51]			140
Puska *et al.*[52]	SC	Atomic superposition	134
Brauer *et al.*[15]	SC	Atomic superposition	141
Brauer *et al.*[16]	SC	TB-LMTO	138
Barbiellini *et al.*[38]	none	LMTO-ASA	124
	GC	LMTO-ASA	139
	none	Atomic superposition	121
	GC	Atomic superposition	134
Panda *et al.*[53]	none	Pseudopotentials	130
	GC	Pseudopotentials	145
Panda *et al.*[54]	GC	Pseudopotentials	145
	GC	LMTO-ASA	138
Kawasuso *et al.*[9]	SC	Pseudopotentials	143

ones of 3*C*-SiC and 6*H*-SiC of around 140 ps.[6,51] When the SC or GC corrections are applied, results in better agreement with experimental values are obtained, especially when the pseudopotentials method is used. It seems that both ways of taking into account the reduced screening can be used in SiC.

We also studied the effect of the approximation used for the electron-electron exchange-correlation interaction on the obtained lifetimes. We performed calculations using LDA and GGA for monovacancies. Results can be seen in Table IV. Each time the equilibrium volume found with the corresponding given method is used. The lifetimes obtained in LDA are only slightly shorter than in GGA as the corresponding lattice parameter is smaller. The type of the electron-electron interaction functional and of the size of the PAW dataset used in calculations affects all the obtained lifetimes. As we showed before in the case of different numbers of valence electrons,

TABLE IV. Comparison of positron lifetimes obtained in 3*C*-SiC for carbon and silicon vacancies. Different schemes, electron-electron exchange-correlation functionals and PAW data sets are used. Relative lifetimes were calculated according to Eq. (7).

	e-e x-c approx.	Si valence electrons	Scheme	Lifetime (ps)	Relative lifetime
Lattice	LDA	4	CONV	149	
Lattice	GGA	4	CONV	153	
Lattice	LDA	12	CONV	144	
Lattice	GGA	12	CONV	148	
V_C	LDA	4	GGGC	211	42%
V_C	GGA	4	GGGC	217	42%
V_C	LDA	12	PSN	195	35%
V_C	GGA	12	PSN	200	35%
V_{Si}	LDA	4	GGGC	224	51%
V_{Si}	GGA	4	GGGC	231	51%
V_{Si}	LDA	12	PSN	227	58%
V_{Si}	GGA	12	PSN	236	59%

these differences have only a slight effect on the ratio between the lifetimes of defects and that of the lattice. Therefore, to be able to correctly compare the results obtained using the various methods, we present not only the absolute lifetimes, but also relative lifetimes τ_{rel}, calculated according to

$$\tau_{rel} = \frac{\tau_{defect} - \tau_{lattice}}{\tau_{lattice}}, \quad (7)$$

where $\tau_{lattice}$ is the lattice lifetime obtained using the same method and parametrization as for the considered defect.

The GGA approximation of the exchange-correlation interaction between electrons yields better estimations for energies than LDA.[55] The best scenario would be to use GGA in both the GGGC and PSN calculations. However, since in the PSN scheme 12 valence electrons have to be considered in the Si PAW data set, using GGA approximation leads to a very high computation cost. As seen in Table IV, the differences in relative positron lifetimes obtained in PSN + GGA and PSN + LDA are smaller than 1%. The absolute lifetimes calculated in PSN + LDA are shorter mainly due to a smaller lattice parameter used. Based on that, we decided to perform PSN calculations in LDA. For the GGGC scheme GGA is used as the computation cost remains reasonable in this case.

Additionally, in the case of the carbon vacancy, we have studied the effect of the initial geometry on the positron localization. In some theoretical studies, it was found that this defect is not a positron trap,[9,52] which is still controversial. To be sure that our result is not a consequence of the starting point, we performed two calculations. In the first one, we started with perfect atomic positions, while in the second one, we began with a vacancy that was already relaxed without a positron. The carbon vacancy itself relaxes inwards in a D_{2d} symmetry,[27] due to formation of dimerlike bonds between silicon atoms surrounding the defect. A smaller volume of V_C could prevent the positron localization. However, both calculations eventually yield an outward relaxation, in similar T_d geometries. It probably means that a positron can break the bonds between silicon atoms. A similar effect was found for a silicon vacancy in Si.[18–20]

IV. RESULTS AND DISCUSSION

A. Charge states of the monovacancies

1. 3C-SiC

Firstly, we studied the formation energies of the V_C, V_{Si}, and $V_C + C_{Si}$ defects with various charge states from −2 to +2 in 3*C*-SiC. The results for the considered defects are presented in Fig. 2. We see that the carbon vacancy is positive for almost all the values of the electron chemical potential. It means that in the 3*C* polytype the V_C defect should be visible in PAS only in strongly *n*-doped samples in which the Fermi level lays close to the conduction-band minimum. The $V_C + C_{Si}$ complex should not be observed at all in 3*C*-SiC using PAS. According to our calculations the silicon vacancy should be detected for almost all types of doping if it is present. However, its formation energy is higher than the one of the $V_C + C_{Si}$ complex for all the electron chemical potentials laying in the gap. V_{Si} is thus metastable in 3*C*-SiC and should not be seen, as was already predicted in previous studies.[23,24]

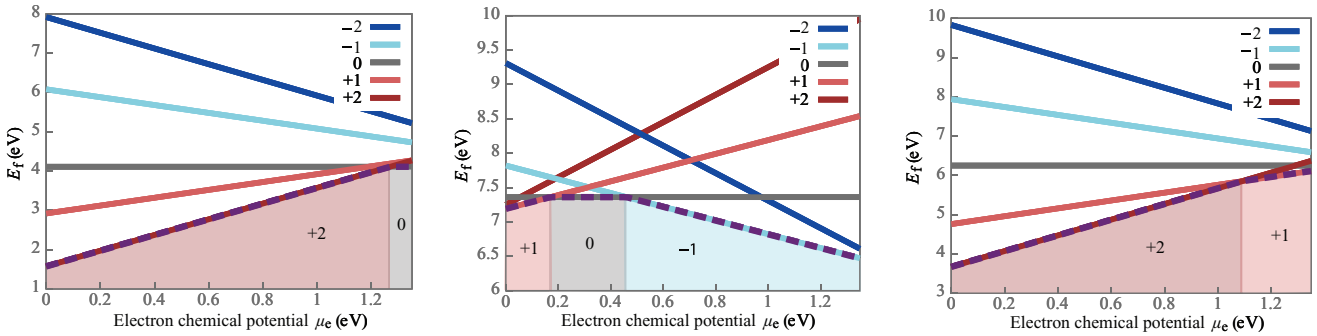

(a) V_C (b) V_{Si} (c) V_C+V_{Si}

FIG. 2. (Color online) Formation energies of various charge states of the three defects studied in 3*C*-SiC.

2. 6*H*-SiC

We also calculated the formation energies for various charge states of various configurations of the three defects in 6*H*-SiC. In this polytype three nonequivalent atomic sites exist, one hexagonal h and two quasicubic, k_1 and k_2, as shown in Fig. 3.

We firstly performed calculations for the three possible carbon monovacancies. Results are presented in Fig. 4. The formation energies for the three sites differ only very slightly. For example, for the neutral defects, we found the formation energy of 4.23 eV at the h site, 4.15 eV at the k_1 site, and 4.10 eV at the k_2 site. Moreover, the general forms of the charge state predominance as a function of μ_e are very similar. In Fig. 4 we compare the results obtained in 6*H*-SiC with the results obtained for 3*C*-SiC, this time plotted up to the edge of the theoretical conduction-band minimum of the 6*H* structure [see Fig. 4(d)]. We see that the results obtained for 6*H*-SiC are very close to the extrapolated results obtained in 3*C*-SiC, especially in the case of the two quasicubic sites. It would be very convenient to be able to predict charge states of the defects in the hexagonal polytype based on the ones obtained in the cubic structure, as the calculations in the latter case are less time consuming.

We compare the charge states of the V_{Si} and $V_C + C_{Si}$ defects in the 6*H* structure with the extrapolated results obtained in 3*C*-SiC. This time we consider only the defects at the hexagonal sites, since it was observed for the carbon vacancy that this case was the most different from the extrapolated results obtained in 3*C*-SiC. Results are presented in Figs. 5 and 6. In the case of the silicon vacancy, we can observe the largest differences. However, as we are mostly interested in the charge state prediction for PAS experiments interpretation, we can consider that the extrapolation of the results obtained in 3*C*-SiC is good enough for our purpose.

As for the defects detectability, the case of 6*H*-SiC is different from the one of 3*C*-SiC. Due to a larger energy gap and higher electron chemical potentials that can be reached, defects can get more negative. In this polytype, the carbon vacancy should be visible in the n-type samples. For the $V_C + C_{Si}$ complex, there is a small region where it should be neutral, hence visible. However, unlike in the case of 3*C*-SiC, the complex is not always stable in 6*H*-SiC compared to V_{Si}. We show in Fig. 7 the areas of stability of V_{Si} and $V_C + C_{Si}$. When the $V_C + C_{Si}$ complex is stable, it is positive and cannot therefore be detected by PAS. In n-doped materials, the silicon vacancy is stable, with at least a double negative charge state. The −3 and −4 charge states of this defect were not considered in our calculations but their existence is highly probable in strongly doped n-type 6*H*-SiC samples.

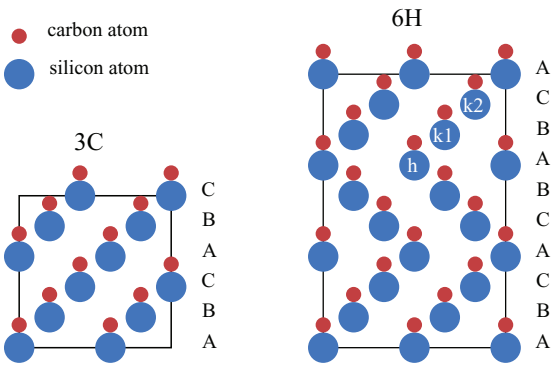

FIG. 3. (Color online) Stacking sequences in the [1120] plane of the two studied polytypes, cubic 3*C* and hexagonal 6*H*. In 6*H*-SiC atoms occupy three different sites: hexagonal h and two quasicubic, k_1 and k_2.

B. Positron lifetimes

1. 3*C*-SiC neutral defects

The three calculations schemes, CONV, GGGC, and PSN, are compared for three neutral monovacancies in 3*C*-SiC. Results are presented in Table V and compared with the lifetimes obtained by Brauer *et al.*[15] Their calculations were done in the conventional scheme including a semiconductor correction. They used the atomic superimposition method in a supercell at the experimental volume, containing 64 atoms and they did not take into account the relaxation effect. Our results show that the lattice lifetime calculated in the PSN scheme is in a better agreement with the experimental one of 140 ps[51] measured for 3*C*-SiC than the one calculated in GGGC. Moreover, we see that in our study, all the defects relax strongly outwards. This leads to much longer lifetimes than the ones predicted by Brauer *et al.* This shows clearly that the effect of the positron on the relaxation cannot be neglected. It can also be observed that the GGGC scheme leads to larger relaxations than PSN. We studied the effect of

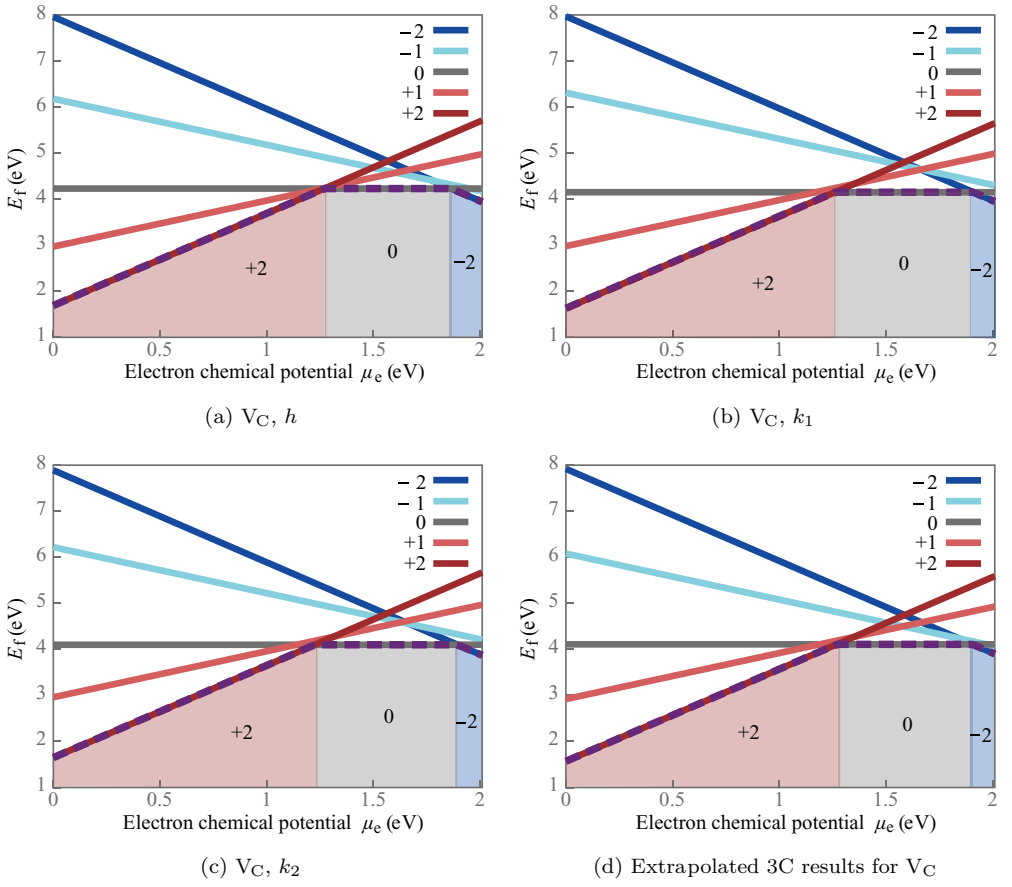

(a) V_C, h (b) V_C, k_1

(c) V_C, k_2 (d) Extrapolated 3C results for V_C

FIG. 4. (Color online) Formation energies of various charge states of the carbon vacancy in 6H-SiC, compared with results obtained in 3C polytype, extrapolated to the 6H-SiC gap end.

the localized positron on the Jahn-Teller distortion. We forced the distortion at the beginning of the calculations for the carbon and silicon vacancies and we observed that it was practically canceled at the end (distortion of less than 1% left in both GGGC and PSN) and the lifetimes were the same as in the perfect T_d geometry, with an accuracy of 1 ps. Binding energies (E_b) between the positron and the defect, i.e., the differences between the positron energies in the lattice and in the defect, were also calculated in the three schemes. They are presented in Table VI. A positive value of E_b means that the positron is trapped in the defect. It can be seen that the conventional scheme does not predict the positron trapping in the carbon vacancy, which is found using the GGGC and PSN schemes. Moreover, we found that GGGC yields much larger binding energies than the two other schemes. This is consistent with the overestimation of the positron localization in this scheme, that

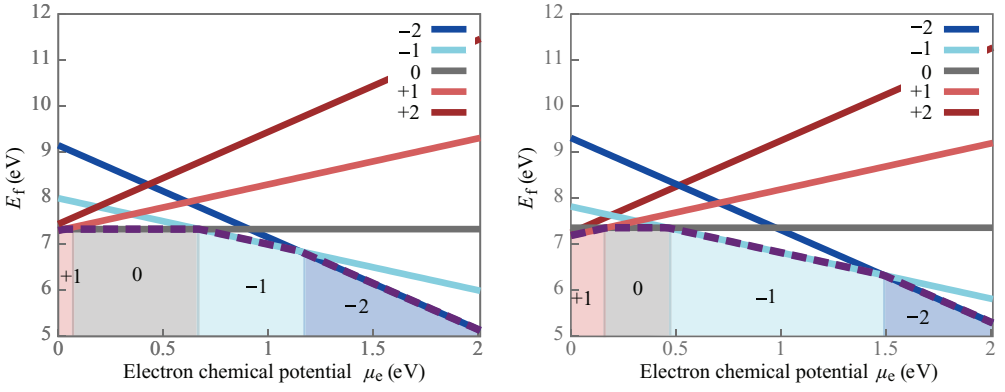

(a) V_{Si}, h (b) Extrapolated 3C results for V_{Si}

FIG. 5. (Color online) Formation energies of various charge states of the silicon vacancy in 6H-SiC, compared with results obtained in 3C polytype, extrapolated to the 6H-SiC gap end.

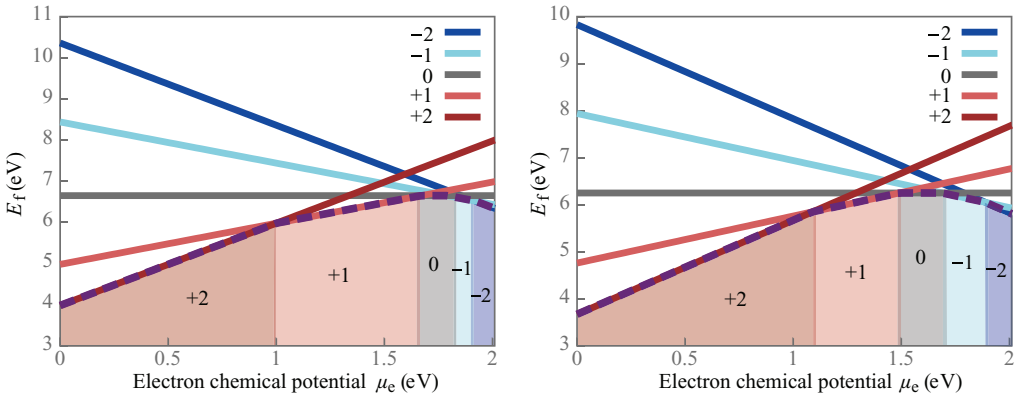

(a) $V_C + C_{Si}$, h-h (b) Extrapolated 3C results for $V_C + C_{Si}$

FIG. 6. (Color online) Formation energies of various charge states of the $V_C + C_{Si}$ complex in 6H-SiC, compared with results obtained in 3C polytype, extrapolated to the 6H-SiC gap end.

was already reported by Car *et al.*[21] Because of this effect, the relaxation predicted in GGGC can be incorrect. Therefore we decided to use the PSN method, which contains more accurate approximations, in further studies.

2. 3C-SiC charged defects

Our study of the various charge states of the defects in silicon carbide showed that the neutral defects should not be the only ones to be observed in the PAS experiments. We thus performed calculations for the negatively charged defects as well. We did not consider positive defects as they should not be observed by this experimental technique. Results are presented in Table VII. The positron lifetimes of the negative vacancies are slightly shorter than for the neutral ones. Firstly, it is because the additional negative charges increase the annihilation rate. Secondly, the additional electrons take part in the bonding and reduce the outwards relaxation. However, the differences between the lifetimes of neutral and negative defects are relatively small (around 5 ps). We also studied the effect of the positron on the Jahn-Teller distortion in the case of charged defects. As in to the case of neutral vacancies, we found that for all charges, even when the distortion was forced at the beginning of the calculations, it was almost completely canceled out at the end (distortion of less than 1 % left) for all the charge states.

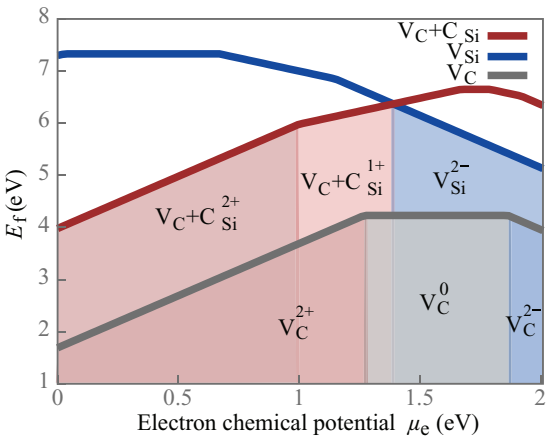

FIG. 7. (Color online) Comparison of the formation energies of three hexagonal defects in 6H-SiC. For $V_C + C_{Si}$ and V_{Si} only the regions where they are stable are colored.

3. 6H-SiC neutral defects

It has been shown in the literature[15,16] that the positron lifetimes of various defects are similar in different polytypes. However, the defect relaxation was not taken into account in the earlier calculations. We performed PSN calculations for selected configurations of the three defects in the hexagonal polytype to verify if the defects free volumes evolve in the same way in 3C-SiC and 6H-SiC. Results are presented in Table VIII. The lattice lifetime obtained for the hexagonal polytype is very close to the one of the cubic structure and in a good agreement with the experimental lifetime of 140 ps[6] obtained for this polytype. We can see from the comparison between Tables V and VIII that the lifetimes of defects at hexagonal sites in 6H-SiC are also very similar to those in 3C-SiC. Additionally, for the silicon vacancy there are only small differences between the three possible sites and relaxations are also similar. For V_C and $V_C + C_{Si}$, however, we find significantly shorter lifetimes when the defect is located at one of the quasicubic sites, which is related to the large differences in the relaxations of k_1-k_1 and k_2-k_2 configurations of $V_C + C_{Si}$. The relaxation induced by the positron makes the first neighbors of the vacancy move relatively far from their perfect positions. However, this outward movement is limited by the second neighbors or even the third neighbors, whose configuration is not the same for each site. The reorganization is different for the two sublattices and this effect is smaller for V_{Si}. This probably explains the differences in lifetimes and relaxations for defects at different sites and the differences with the 3C-SiC case. In the case of the carbon vacancy, as the positron lifetimes of the various configurations are not the same, and all of them can be present in the material and the PAS signals will be mixed.

TABLE V. Calculated positron lifetimes in 3*C*-SiC compared with the results of Brauer *et al.*[15] Results were obtained for unrelaxed vacancies in the CONV scheme and relaxed vacancies in the GGGC and PSN schemes. Atomic relaxations are calculated as a relative change in distances between the first neighbors of the defect compared to the perfect defect. Relative lifetimes, computed as in Eq. (7), are given in parentheses.

	Lifetime CONV	Lifetime Ref. 15	Lifetime GGGC	Relaxation GGGC	Lifetime PSN	Relaxation PSN
a_{cell}	4.39 Å	4.36 Å	4.39 Å	4.39 Å	4.33 Å	4.33 Å
Valence states Si	3*s*, 3*p*		3*s*, 3*p*	3*s*, 3*p*	2*s*, 2*p*, 3*s*, 3*p*	2*s*, 2*p*, 3*s*, 3*p*
Lattice	153	138	153		144	
V_C	154 (1%)	153 (11%)	217 (42%)	+17%	195 (35%)	+12%
V_{Si}	198 (28%)	191 (38%)	231 (51%)	+12%	227 (58%)	+12%
$V_C + C_{Si}$	170 (11%)	–	217 (42%)	+27% C-Si +9% Si-Si	203 (41%)	+21% C-Si +7% Si-Si

4. 6*H*-SiC charged defects

We also performed positron lifetime calculations for negative monovacancies in 6*H*-SiC. We considered carbon and silicon vacancies with a −2 charge state as these were the only negative defects that should be detected by PAS in this polytype according to our formation energies study. Results are presented in Table IX. Positron lifetimes of all V_{Si} configurations and for the two quasicubic types of V_C are only slightly shorter than for the neutral defects. It is similar to the case of 3*C*-SiC. The lifetime of the negative hexagonal carbon vacancy is 13 ps shorter than for the neutral one (shown in Table VIII), which is caused by a much smaller outward relaxation of this particular defect.

V. COMPARISON WITH EXPERIMENTS

Finally, we compare our results with the experimental data available in literature. In n-doped, irradiated 3*C*-SiC a signal varying with temperature from 210 ps up to 220 ps was detected by Kerbiriou *et al.*[56] The authors concluded that the lifetimes were coming from at least two vacancy-type defects: V_{Si} and $V_C + V_{Si}$. This identification, however, was based on the calculation results by Brauer *et al.*,[15,16] which did not take into account the effect of the defect relaxation or its charge state. The variation of the lifetime with temperature implies the presence of a defect that changes its charge state, or at least two defects, among which one is negative or changes its charge state. Kerbiriou *et al.* also examined the sample using electron paramagnetic resonance (EPR) and identified the T1 signal, attributed to V_{Si}^{1-} (see Ref. 56–59). Considering the calculations results presented here, we firstly verified whether the defect corresponding to the experimental lifetime could be the silicon vacancy changing its charge state. The shortest lifetime that we obtained for this defect in 3*C*-SiC yields 222 ps (V_{Si}^{2-}). However, as the experimental lifetime for the lattice is shorter than the one we calculated (140 ps and 144 ps, respectively), we have to consider the lifetime relative to the experimental one. It yields 216 ps ($\frac{222\text{ ps}\,140\text{ ps}}{144\text{ ps}}$) for V_{Si}^{2-}. This lifetime is longer than the one of 210 ps observed by Kerbiriou *et al.* at low temperatures. Additionally, the change of the charge state of the silicon vacancy would result in a change in the EPR signal, while it was found to be the same at all the measurement temperatures. We propose, hence, a second interpretation: the positron lifetime observed by Kerbiriou *et al.* comes from both the neutral carbon monovacancy and the negative silicon vacancy. V_C could not be detected by EPR, as it is nonparamagnetic. As temperature increases, the electron chemical potential of the *n*-type material decreases and the carbon vacancies become positive and cannot be detected by PAS any longer. This induces an increase in the lifetime, which becomes closer to the 225 ps (218 ps when scaled to $\tau_{lattice}^{exp.}$) that was calculated for V_{Si}^{1-}.

In the second study on irradiated *n*-type 3*C*-SiC performed by Kawasuso *et al.*,[51] a lifetime component of 188 ps was detected and attributed to the silicon vacancy. The same T1 signal, indicating the presence of V_{Si} was detected by EPR in the same sample. The lifetime itself is close to the one that

TABLE VI. Binding energies between the positron and the defect calculated in various schemes as in Ref. 22. Results were obtained for unrelaxed vacancies in the CONV scheme and relaxed vacancies in the GGGC and PSN schemes. Positive values mean positron trapping.

	E_b CONV (eV)	E_b GGGC (eV)	E_b PSN (eV)
V_C	−0.18	+2.65	+1.07
V_{Si}	+2.41	+5.07	+2.08
$V_C + C_{Si}$	+0.89	+3.82	+1.61

TABLE VII. Calculated positron lifetimes of negative and neutral monovacancies in 3*C*-SiC. Results obtained in the PSN scheme are presented. Relative lifetimes, computed as in Eq. (7), are given in parentheses.

	Lifetime PSN (ps)	Relaxation PSN
Lattice	144	
V_C^0	195 (35%)	+12%
V_C^{1-}	193 (34%)	+10%
V_C^{2-}	188 (31%)	+10%
V_{Si}^0	227 (58%)	+12%
V_{Si}^{1-}	225 (56%)	+11%
V_{Si}^{2-}	222 (54%)	+11%

TABLE VIII. Positron lifetimes and atomic relaxations calculated in the PSN scheme. Selected defects of the 6*H* polytype are considered. Relative lifetimes, computed as in Eq. (7), are given in parentheses. The relaxation indicated is calculated as the average relative change in distance between the first neighbors of the defect.

	Site	Lifetime PSN (ps)	Relaxation PSN
Lattice		143	
V_C	h	193 (35%)	+12%
V_C	k_1	175 (22%)	+5%
V_C	k_2	173 (21%)	+6%
V_{Si}	h	226 (58%)	+11%
V_{Si}	k_1	226 (58%)	+12%
V_{Si}	k_2	226 (58%)	+12%
$V_C + C_{Si}$	h-h	204 (43%)	+18% C-Si +6% Si-Si
$V_C + C_{Si}$	k_1-k_1	202 (41%)	+18% C-Si +4% Si-Si
$V_C + C_{Si}$	k_2-k_2	188 (31%)	+11% C-Si +6% Si-Si

we calculated for the carbon vacancy, but we cannot explain the simultaneous existence of these PAS and EPR signals. The study of Kawasuso *et al.* was performed only at room temperature, hence the charge state of the observed defect is not known and it is not certain whether the signal comes from one or several defect types. Additionally, the experiment of Kawasuso *et al.* was carried out on a 30 μm 3*C*-SiC sample supported on unirradiated 6*H*-SiC. It is hence possible that even though the silicon vacancies were created in the 3*C*-SiC layer, the positron lifetime observed was also affected by the supporting material. In any case, since not many experimental data have been published for 3*C*-SiC it is rather difficult to draw definitive conclusions on the defects present based on the positron lifetimes alone. Moreover, we found that there is only a small region close to the conduction band where the carbon vacancy should be neutral and detected by PAS. The electron chemical potential changes with temperature and irradiation and is difficult to determine precisely. Thus, it is complicated to predict whether the carbon vacancies should be detected in a given 3*C*-SiC sample, therefore to interpret the PAS results in this polytype.

TABLE IX. Calculated positron lifetimes of monovacancies with a −2 charge state in 6*H*-SiC. Results obtained in the PSN scheme are presented. Relative lifetimes, computed as in Eq. (7), are given in parentheses.

	Site	Lifetime PSN (ps)	Relaxation PSN
Lattice		143	
V_C^{2-}	h	180 (26%)	+6%
V_C^{2-}	k_1	170 (19%)	+2%
V_C^{2-}	k_2	171 (20%)	+3%
V_{Si}^{2-}	h	222 (55%)	+10%
V_{Si}^{2-}	k_1	223 (56%)	+11%
V_{Si}^{2-}	k_2	222 (55%)	+10%

Concerning 6*H*-SiC, no defects are observed by PAS in *p*-type samples in the majority of studies.[5,6,12] As for the *n*-type 6*H*-SiC, several group of lifetimes are observed, two of which are in the range of our calculated lifetimes. Shorter experimental positron lifetimes, of 176,[13], 183,[12] 174, and 176 ps[14] were observed and assigned to the silicon vacancy using the calculations of Brauer *et al.* These lifetimes are, however, much smaller than the lifetimes we calculated for both V_{Si}^0 (226 or 221 ps when scaled to $\tau_{lattice}^{exp.}$) and V_{Si}^{-2} (222 and 223 ps or 217 and 218 ps scaled to $\tau_{lattice}^{exp.}$). These experimental lifetimes are on the contrary in a very good agreement with the ones we obtained for the neutral carbon vacancy (175, 173, and 193 ps or 171, 169, and 189 ps when scaled to $\tau_{lattice}^{exp.}$).

The second group of experimental lifetimes observed in *n*-type 6*H*-SiC contains lifetimes of 210,[13] 202,[6] 210, and 220 ps.[5] These signals are between the values we calculated for V_C and V_{Si}. Since for vacancy complexes longer lifetimes are expected, we assume that these can be mixed signals of the carbon and silicon monovacancies.

The positron lifetimes that we obtained for the fully relaxed monovacancies in SiC differ strongly than those calculated previously for the perfect defects. These results can therefore affect the PAS experiments interpretations, which should be reconsidered. Consistency of our results with complementary defect characterization methods should be evaluated. However, as the monovacancies are not the only defects which can be formed by irradiation in SiC, calculations should be also done for vacancy complexes. In addition, in some cases the theoretical positron lifetimes alone do not seem to permit the interpretation of the experimental data. The calculations of momentum distribution of annihilating electron-positron pairs (Doppler broadening) for relaxed defects in SiC could then be of interest.

VI. CONCLUSIONS

We investigated the positron lifetimes of V_C, V_{Si}, and $V_C + C_{Si}$ in 3*C*-SiC and 6*H*-SiC using three calculations schemes, CONV, GGGC, and PSN and taking into account the atomic relaxation. We showed that the most accurate PSN scheme should be used to describe correctly the positron annihilation characteristics in SiC. We also performed formation energy calculations for the three monovacancies for various charge states from −2 to +2.

We found that in the 3*C* polytype none of these defects should be seen in PAS, except the carbon vacancy in strongly *n*-doped samples. In 6*H*-SiC, neutral or negative V_C and a negative V_{Si}, with at least a −2 charge, should be observed. These defects, however, should be observed only in *n*-type samples. For lower electron chemical potentials, the carbon vacancy is positive and the silicon vacancy is metastable. The complex that V_{Si} transforms into—$V_C + C_{Si}$—is always positive according to our calculations. Thus it should not be observed by PAS.

We show also that the charge state predominance of the defects in the 6*H* polytype can be predicted through the extrapolation of the results obtained for 3*C*. It is very convenient as the calculations are easier and less time-consuming in the

cubic structure. Our charge state calculations are in a good agreement with the experimental results, as in the majority of PAS studies on SiC, no defects are seen in p-type samples.

The positron lifetimes obtained in the present study differ strongly from the calculated lifetimes reported before. They are much longer, mainly due to a significant increase of the defect volumes caused by the atomic relaxation. The changes in atomic positions cannot therefore be neglected in positronic calculations for silicon carbide. As the previous calculations, using less accurate approximations, were often used for the interpretation of PAS experimental results, we suggest that defect identifications should be reconsidered.

ACKNOWLEDGMENTS

This research was supported by the basic research program on nuclear materials of the Nuclear Energy Division at CEA, MATAV. This work was partly performed using HPC resources from GENCI-CCRT (Grant No. 2012096961). The authors are grateful to Marie-France Barthe, Michel Freyss, and Emerson Vathonne for insightful discussions.

APPENDIX: ENHANCEMENT FACTORS FOR SEMICONDUCTORS

1. CONV and GGGC schemes

The enhancement factor including the semiconductor correction used in the CONV and GGGC schemes was proposed by Puska.[37] It takes the form

$$g(n) = \pi c r_0^2 n\Big[1 + 1.23r_s + 0.8295r_s^{3/2} - 1.26r_s^2 + 0.3286r_s^{5/2} + \frac{1}{6}(1 - 1/\epsilon_\infty)r_s^3\Big], \quad \text{(A1)}$$

where c is the speed of light, r_0 is the classical radius of an electron, and r_s, in atomic units, is a density parameter equal to the radius of a sphere containing one electron:

$$\frac{4}{3}\pi r_s^3 n = 1, \quad \text{(A2)}$$

for a electronic density n.

2. PSN scheme

In the PSN scheme, the enhancement factor g depends on both the electron and the positron densities. Its formulation was firstly proposed by Boroński and Nieminen,[34] but in our study we used the parametrization by Puska, Seitsonen, and Nieminen.[22] The factor is defined as

$$g(n^+,n) = a(n_>)n_<^3 + b(n_>)n_<^2 + c(n_>)n_< + g_0(n_>), \quad \text{(A3)}$$

where $n_>$ and $n_<$ stand for the positron or electron density, depending on which is larger and smaller, respectively. The parametrizing functions $a(n)$, $b(n)$, and $c(n)$ are expressed as

$$a(n) = \frac{1}{n^3}[2k(n) - 6g_1(n) + 8g_2(n) - 2g_0(n)], \quad \text{(A4)}$$

$$b(n) = \frac{1}{n^2}[-3k(n) + 11g_1(n) - 16g_2(n) + 5g_0(n)], \quad \text{(A5)}$$

and

$$c(n) = \frac{1}{n}[k(n) - 4g_1(n) + 8g_2(n) - 4g_0(n)]. \quad \text{(A6)}$$

The function $k(n)$ reads

$$k(n) = \frac{1}{2}n\frac{\mathrm{d}}{\mathrm{d}n}g_1(n). \quad \text{(A7)}$$

The $g_0(n)$, $g_1(n)$, and $g_2(n)$ are the functions interpolating and extrapolating the data obtained by Lantto in the hypernetted-chain approximation of the many-body theory.[60]

To take into account the semiconductor correction in the PSN scheme, we modified functions $g_0(n)$, $g_1(n)$, and $g_2(n)$, in analogy to what was done in the $g(n)$ factor of CONV and GGGC. As a result, the interpolating functions occurring in the model of Puska *et al.*, now expressed as a function of r_s, take the form

$$g_0(r_s) = 1 + 1.2300r_s + 0.9889r_s^{3/2} - 1.4820r_s^2 + 0.3956r_s^{5/2} + \tfrac{1}{6}(1 - 1/\epsilon_\infty)r_s^3, \quad \text{(A8)}$$

$$g_1(r_s) = 1 + 2.0286r_s - 3.3892r_s^{3/2} - 3.0547r_s^2 - 1.0540r_s^{5/2} + \tfrac{1}{6}(1 - 1/\epsilon_\infty)r_s^3, \quad \text{(A9)}$$

and

$$g_2(r_s) = 1 + 0.2499r_s + 0.2949r_s^{3/2} + 0.6944r_s^2 - 0.5339r_s^{5/2} + \tfrac{1}{6}(1 - 1/\epsilon_\infty)r_s^3, \quad \text{(A10)}$$

with

$$\frac{4}{3}\pi r_s^3 n = 1. \quad \text{(A11)}$$

It has to be noted, that this modification is done only when the electron density is higher than the one of the positron, i.e., when it enters Eq. (A3) as $n_>$. When the positron density is the larger one, the functions $g_0(n)$, $g_1(n)$, and $g_2(n)$ keep their original form with $1/\epsilon_\infty = 0$.

*julia.wiktor@cea.fr

[1] P. Yvon and F. Carré, J. Nucl. Mater. **385**, 217 (2009).
[2] L. Giancarli, M. Ferrari, M. Fütterer, and S. Malang, Fusion Eng. Des. **4950**, 445 (2000).
[3] M. Willander, M. Friesel, Q. Wahab, and B. Straumal, J. Mater. Sci.: Mater. Electron. **17**, 1 (2006).
[4] M.-F. Barthe, D. T. Britton, C. Corbel, A. Hempel, L. Henry, P. Desgardin, W. Bauer-Kugelmann, G. Kögel, P. Sperr, and W. Triftshäuser, Physica B **308-310**, 668 (2001).
[5] S. Arpiainan, K. Saarinen, P. Hautojärvi, L. Henry, M.-F. Barthe, and C. Corbel, Phys. Rev. B **66**, 075206 (2002).

[6]L. Henry, M.-F. Barthe, C. Corbel, P. Desgardin, G. Blondiaux, S. Arpiainen, and L. Liszkay, Phys. Rev. B **67**, 115210 (2003).
[7]C. C. Ling, C. D. Beling, and S. Fung, Phys. Rev. B **62**, 8016 (2000).
[8]C. C. Ling, A. H. Deng, S. Fung, and C. D. Beling, Appl. Phys. A **70**, 33 (2000).
[9]A. Kawasuso, M. Yoshikawa, H. Itoh, R. Krause-Rehberg, F. Redmann, T. Higuchi, and K. Betsuyaku, Physica B **376-377**, 350 (2006).
[10]C. H. Lam, T. W. Lam, C. C. Ling, S. Fung, C. D. Beling, H. De-Sheng, and W. Huimin, J. Phys.: Condens. Matter **16**, 8409 (2004).
[11]C. Lam and C. Ling, Nucl. Instrum. Methods B **251**, 479 (2006).
[12]A. Kawasuso, H. Itoh, S. Okada, and H. Okumura, J. Appl. Phys. **80**, 5639 (1996).
[13]A. A. Rempel, W. Sprengel, K. Blaurock, K. J. Reichle, J. Major, and H.-E. Schaefer, Phys. Rev. Lett. **89**, 185501 (2002).
[14]S. Dannefaer and D. Kerr, Diamond Relat. Mater. **13**, 157 (2004).
[15]G. Brauer, W. Anwand, P. G. Coleman, A. P. Knights, F. Plazaola, Y. Pacaud, W. Skorupa, J. Störmer, and P. Willutzki, Phys. Rev. B **54**, 3084 (1996).
[16]G. Brauer, W. Anwand, E.-M. Nicht, J. Kuriplach, M. Šob, N. Wagner, P. G. Coleman, M. J. Puska, and T. Korhonen, Phys. Rev. B **54**, 2512 (1996).
[17]T. E. M. Staab, L. M. Torpo, M. J. Puska, and R. M. Nieminen, Mater. Sci. Forum **353**, 533 (2000).
[18]M. Saito and A. Oshiyama, Phys. Rev. B **53**, 7810 (1996).
[19]I. Makkonen, M. Hakala, and M. J. Puska, Phys. Rev. B **73**, 035103 (2006).
[20]I. Makkonen and M. J. Puska, Phys. Rev. B **76**, 054119 (2007).
[21]L. Gilgien, G. Galli, F. Gygi, and R. Car, Phys. Rev. Lett. **72**, 3214 (1994).
[22]M. J. Puska, A. P. Seitsonen, and R. M. Nieminen, Phys. Rev. B **52**, 10947 (1995).
[23]M. Bockstedte, A. Mattausch, and O. Pankratov, Phys. Rev. B **68**, 205201 (2003).
[24]F. Bruneval and G. Roma, Phys. Rev. B **83**, 144116 (2011).
[25]M. J. Puska and R. M. Nieminen, Rev. Mod. Phys. **66**, 841 (1994).
[26]S. B. Zhang and J. E. Northrup, Phys. Rev. Lett. **67**, 2339 (1991).
[27]A. Zywietz, J. Furthmüller, and F. Bechstedt, Phys. Rev. B **59**, 15166 (1999).
[28]M. Leslie and N. J. Gillan, J. Phys. C **18**, 973 (1985).
[29]S. Lany and A. Zunger, Model. Simul. Matter. Sci. Eng. **17**, 084002 (2009).
[30]S. E. Taylor and F. Bruneval, Phys. Rev. B **84**, 075155 (2011).
[31]Y. Goldberg, in *Properties of Advanced Semiconductor Materials GaN, AlN, InN, BN, SiC, SiGe* edited by M. E. Levinshtein, S. L. Rumyantsev, and M. S. Shur (Wiley, New York, 2001).
[32]H.-P. Komsa, T. T. Rantala, and A. Pasquarello, Phys. Rev. B **86**, 045112 (2012).
[33]P. Deák, A. Gali, B. Aradi, and T. Frauenheim, Phys. Status Solidi B **248**, 790 (2011).
[34]E. Boroński and R. M. Nieminen, Phys. Rev. B **34**, 3820 (1986).
[35]J. Arponen and E. Pajanne, J. Phys. F **9**, 2359 (1979).
[36]R. M. Nieminen, E. Boroński, and L. J. Lantto, Phys. Rev. B **32**, 1377 (1985).
[37]M. J. Puska, J. Phys.: Condens. Matter **3**, 3455 (1991).
[38]B. Barbiellini, M. J. Puska, T. Korhonen, A. Harju, T. Torsti, and R. M. Nieminen, Phys. Rev. B **53**, 16201 (1996).
[39]M. Torrent, F. Jollet, F. Bottin, G. Zérah, and X. Gonze, Comput. Mat. Sci. **42**, 337 (2008), http://www.abinit.org.
[40]X. Gonze *et al.*, Comput. Phys. Commun. **180**, 2582 (2009), http://www.abinit.org.
[41]P. E. Blöchl, Phys. Rev. B **50**, 17953 (1994).
[42]N. A. W. Holzwarth, A. R. Tackett, and G. E. Matthews, Comput. Phys. Commun. **135**, 329 (2001).
[43]J. P. Perdew, K. Burke, and M. Ernzerhof, Phys. Rev. Lett. **77**, 3865 (1996).
[44]C. G. Broyden, J. Inst. Math. Appl. **6**, 221 (1970).
[45]R. Fletcher, Comput. J. **13**, 317 (1970).
[46]D. Goldfarb, Math. Comput. **24**, 23 (1970).
[47]D. F. Shanno, Math. Comput. **24**, 647 (1970).
[48]L. Patrick and W. J. Choyke, Phys. Rev. B **2**, 2255 (1970).
[49]H. Takenaka and D. J. Singh, Phys. Rev. B **77**, 155132 (2008).
[50]G. Jomard and M. Torrent (unpublished).
[51]A. Kawasuso, H. Itoh, N. Morishita, M. Yoshikawa, T. Ohshima, I. Nashiyama, S. Okada, H. Okumura, and S. Yoshida, Appl. Phys. A **67**, 209 (1998).
[52]M. J. Puska, S. Mäkinen, M. Manninen, and R. M. Nieminen, Phys. Rev. B **39**, 7666 (1989).
[53]B. K. Panda, W. LiMing, S. Fung, and C. D. Beling, Phys. Rev. B **56**, 7356 (1997).
[54]B. K. Panda, G. Brauer, W. Skorupa, and J. Kuriplach, Phys. Rev. B **61**, 15848 (2000).
[55]W. Koch and M. C. Holthausen, *A Chemist's Guide to Density Functional Theory* (Wiley-VCH, 2000).
[56]X. Kerbiriou, M.-F. Barthe, S. Esnouf, P. Desgardin, G. Blondiaux, and G. Petite, J. Nucl. Mater. **362**, 202 (2007).
[57]H. Itoh, M. Yoshikawa, I. Nashiyama, S. Misawa, H. Okumura, and S. Yoshida, IEEE Trans. Nucl. Sci. **37**, 1732 (1990).
[58]X. Kerbiriou, M.-F. Barthe, S. Esnouf, P. Desgardin, G. Blondiaux, and E. Balanzat, Nucl. Instrm. Meth. B **250**, 259 (2006).
[59]J. Lefèvre, J.-M. Costantini, D. Gourier, S. Esnouf, and G. Petite, Phys. Rev. B **83**, 075201 (2011).
[60]L. J. Lantto, Phys. Rev. B **36**, 5160 (1987).